Strathclyde Engagement with the National HVDC Centre: Assessment and Mitigation of Converter Interactions

Doc. Type: Technical Report		*Date:* **19/02/2020**	
Doc. N°: **USTRATH-HVDC Centre-P2-002**		*Issue:* **2**	*Page:* **1** *of* **23**
Title: Development of typical AC network configuration for converter interaction study			

	Name& Function	*Signature*	*Date*
Prepared by:	Deyang Guo, Yin Chen, Lie Xu, University of Strathclyde		18/02/2020
Approved by:	Agusti Egea, University of Strathclyde		19/02/2020
Authorized by:	Ben Marshall, The National HVDC Centre		03/07/2020
Accepted by:	Simon Marshall, The National HVDC Centre		03/07/2020

DISTRIBUTION LIST	N	A	I
Internal			
External			
N=Number of copy A=Application I=Information			

TABLE OF CONTENT

Executive summary

This report describes the work carried out on developing a suitable AC network model for converter interaction and stability analysis. A simplified GB network model based on the previously developed 8-bus dynamic network model representing the power flows among the different GB network zones, is assessed first. The principles of admittance measurement in the positive/negative sequence (PN) frame using frequency sweep in RTCAD time domain simulation is described. The results reveal that, for the existing AC network model with large synchronous generators, the measured admittances in the PN frame are largely inductive with negligible cross coupling effects between the P and N axes. The dynamics of the synchronous generators and their controls do not affect the admittances of the system seen at the converter connection point due to the fact that their impact frequency (below ten hertz) is much lower than the frequency of interest for converter stability (from tens hertz to hundreds hertz).

Four different load models provided by RSCAD, i.e., constant power load, polynomial load, ZIP load and exponential load, are also considered and their impact on measured network admittance investigated. The results show that different load models present almost identical results due to the large time constant used in RSCAD simulation (0.01s) for determining the variation of load impedance. Thus the traditional method used for load modelling in power system simulation cannot provide adequate dynamic response required for frequency domain converter interaction analysis.

The impact of AC cables on network impedance/admittance is studied using different cable modelling methods. Using the well-recognised frequency dependant AC cable model, the measured network admittances show resonances for long cables, and the longer the AC cable, the lower the resonance frequency. Analytical stability study considering AC cables requires simplified AC cable models, e.g. the lumped PI section model. It is found that PI section based cable model with typical RLC values directly calculated using the Cigre guidebook results in significant errors when compared with frequency dependent cable model. Such errors can be corrected by modifying the calculated capacitance considering the difference between the observed resonant frequencies when the two different cables models are used.

A simplified network structure which can be configured to adopt the concept of multi-infeed interaction factor (MIIF) is proposed for investigating interactions between two converters. The proposed network can reflect the overall network condition of the connecting network, and by reconfiguring the impedances between the converters and the common connection point, different MIIF scenarios can be emulated to reflect real case converter interactions.

1 General introduction

The increase in converter-interfaced renewable sources and HVDC transmission links is significantly changing the characteristics of the GB grid. The dynamics of converters and associated controls of multiple converters located in close vicinities can result in coupled effects among the converters and the connected power networks, which could potentially lead to oscillations across a wide frequency range. Accurate assessment of potential system interactions is critical for ensuring stable operation of future and evolving GB network. Report 1 [1] has described the development of accurate small signal frequency domain models of MMC converters for stability analysis. The aim of this present document is to develop a suitable AC network representation so the measured impedance/admittance is suitable for carrying out frequency domain analysis on multiple converter interaction study.

A RTDS 8-bus dynamic network model was previously developed at Strathclyde in collaboration with GB TSOs to represent dynamic performance of the simplified GB network. This network model is utilised to extract typical admittances seen by connecting HVDC converters using frequency sweep technique based on time-domain RSCAD simulation.

As the main frequency range of concern for converter interaction falls within the frequency range of typical AC cable dynamics, the impact of connection AC cable on network impedance/admittance and system stability need to be examined. It is well-recognised that frequency dependant AC cable model can provide accurate dynamics of cables in time-domain simulation but is not suitable for frequency domain analytical studies due to its complexity. Therefore, cable modelling method and the impact of AC cable length on network admittance need to be fully investigated to ensure simplified cable representation can be used in analytical studies with adequate accuracy.

To carry out frequency domain analytical studies considering multiple converter interaction, a simplified network model is required which can represent the overall network condition at the common connection point, and the electrical interaction/coupling between the converters.

The following sections provide step-by-step development of the simplified network impedance model. Various discoveries during the course of the work related to network modelling are described and corresponding recommendations are proposed to address some of the issues identified.

2 The Simplified UK AC grid model

2.1 Introduction to the existing network model

The existing simplified UK AC grid model is based on real power flow data of the eight areas as presented in the Electricity Ten Year Statement (ETYS) of the UK National Grid (NG) [1] [2]. The AC grid model includes 5 regions of the UK as shown in Figures 1 (a) and (b), where each region is represented by an AC generator and a dynamic load. The model is developed in RTDS as a simplified 8-bus aggregated dynamic model representing key generation and load areas as shown in Figure 2. Each AC generator is modelled as an aggregated large synchronous machine with a step-up transformer (13.8kV/400kV) to represent the generation at the related area. The rating of each generator is set according to the UK 2017 load flow [2].

Each generator is controlled by the generic IEEE ST1 static type excitation system as given in Figure 3 [3] [4]. The generator and excitation system data are obtained from [4]. Also, a GAST gas turbine and speed governor model as shown in Figure 4 are added to each generator to control the speed and input torque to the machine. The load share between the generators is controlled by adjusting the load-frequency references of the governors. The gas turbine model parameters are also obtained from [4].

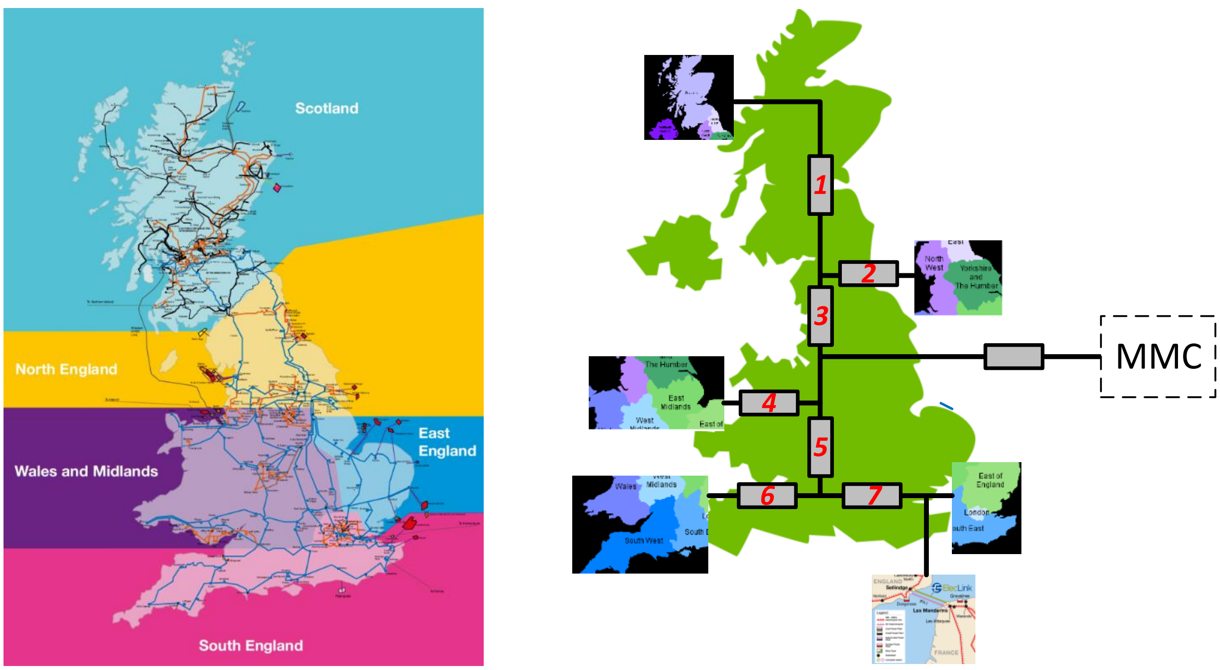

(a) (b)

Figure 1 (a) Regional map of the UK Electricity Transmission System; and (b) Simplified 8-bus GB network representation

The AC overhead transmission lines of the AC grid are modelled using PI-section line models with lumped resistance (R), capacitance (C), and inductance (L). The line parameters (R, C and L) are calculated from the power flow data (P, Q, |V| and voltage angle) provided by the NG ETYS for 2017 [2]. The same methodology for modelling UK transmission system as presented in [5] is used which calculates the line parameters based on the required power flow at each bus.

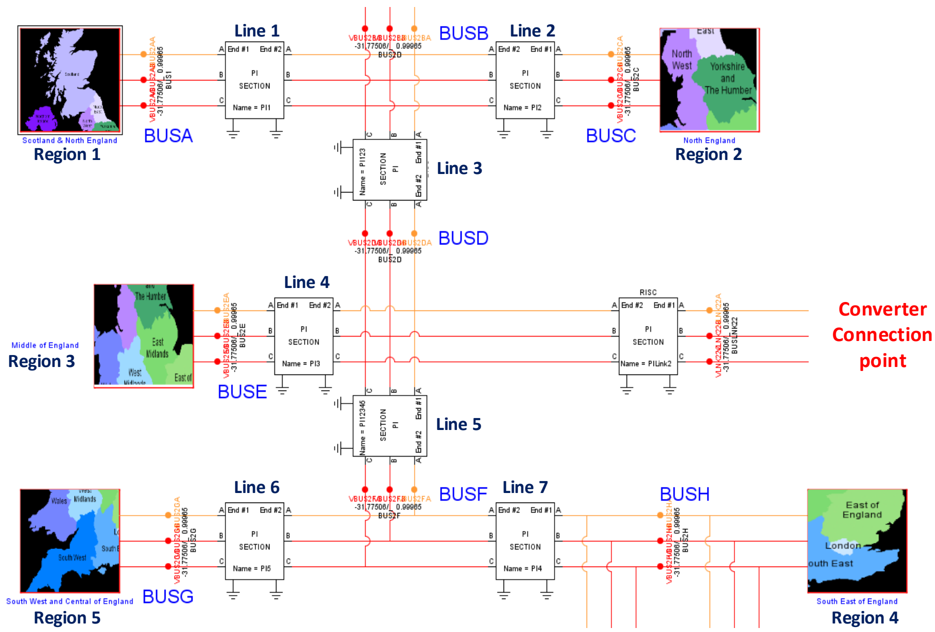

Figure 2 The 8-bus network model implemented in RTDS

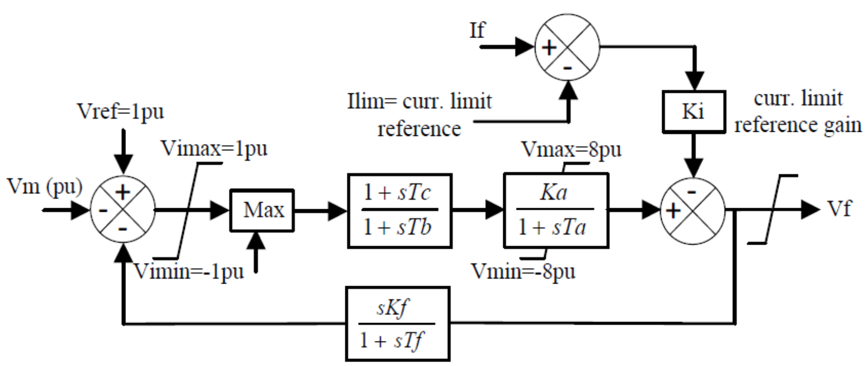

Figure 3 ST1A static excitation system model [3]

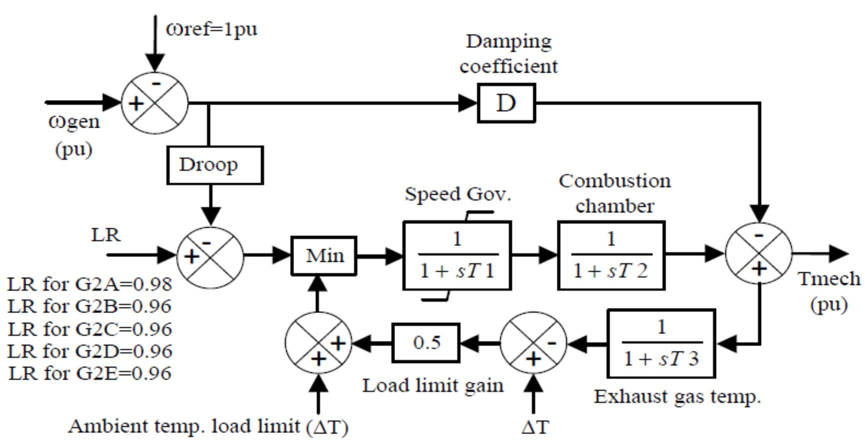

Figure 4 GAST gas turbine and speed governor model [3]

2.2 System parameter of the grid model

The parameters of the generators, loads and transmission lines of the model shown in Figure 2 are listed in Table 1, 2, and 3, respectively. The loads in the RTDS model are modelled as constant power loads whose P and Q are pre-specified. Thus, the simulation calculates the admittance of each load at every time step considering the voltage magnitude at the load terminal.

Table 1 Parameter of the generators (per unit values base on rated voltage of 13.8kV)

	Rated MVA	X_a	X_d	X_d’	X_q	X_q’	R_a	T_{d0}’	T_{d0}’’
G1	11000	0.20	2.3	0.4	2.3	\	0.001	10	0.05
G2	20000	0.20	2.3	0.4	2.3	\	0.001	10	0.05
G3	9160	0.20	2.3	0.4	2.3	\	0.001	10	0.05
G4	14980	0.11	2.3	0.4	2.3	\	0.005	10	0.05
G5	5500	0.20	2.3	0.4	2.3	\	0.005	10	0.05

Table 2 Parameter of the loads

Regions	SG active power setting (MW)	Load	
		Active power (MW)	Reactive power (MVar)
Region 1	9350	8486	4110
Region 2	14200	12548	6077
Region 3	8794	8398	4067
Region 4	14530	17852	10005
Region 5	5500	4150	1041

Table 3 Parameters of the transmission lines (at 50 Hz)

Lines	Resistance (ohms)	Inductive reactance at 50Hz (ohms)	Capacitive reactance at 50 Hz (Mega ohms)
Line 1	2.030	25.024	0.078
Line 2	0.838	11.222	0.037
Line 3	0.007	6.232	0.007
Line 4	4.800	48.500	1.000
Line 5	0.007	6.232	0.007
Line 6	0.007	4.232	0.080
Line 7	2.816	26.122	0.080

2.3 Implementation of the network and converter model in RSCAD

In order to measure the network admittance at a specific operating point, the previously developed AC network model is connected to a MMC model in RSCAD as shown in Figure 5. The MMC RTDS model has its DC side connected to a DC source [6]. The MMC transfers 1000MW active power to the AC grid at unity power factor. The T-line (15 km cable) connects the network model and MMC model which are implemented in two different RTDS racks. The admittance/length of the T-line can be varied to represent the different connection distances of the converter from the network. The steady-state load flow of the AC network model is shown in Table 4.

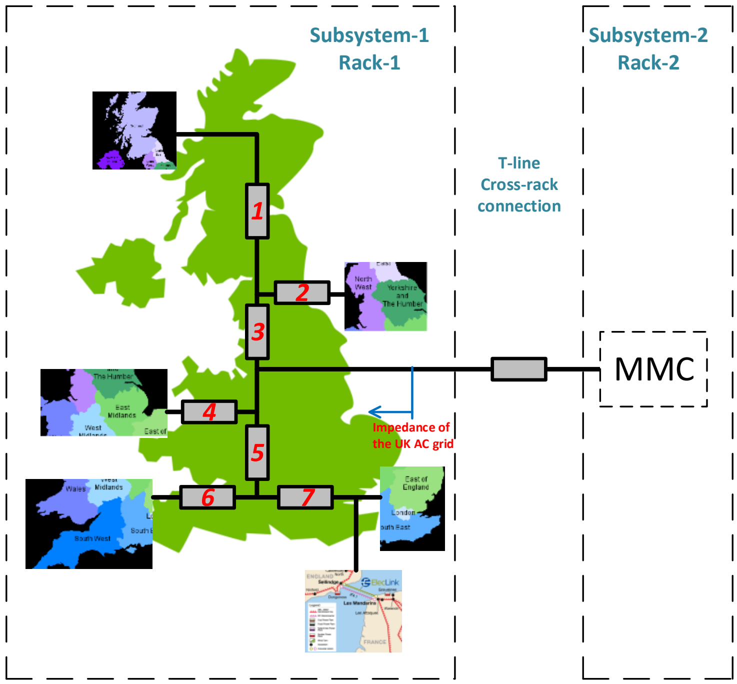

Figure 5 RSCAD implementation of the AC network and MMC models

Table 4 Load flow in the simplified UK AC grid model

	G1	G2	G3	G4	G5	Line 1	Line 2	Line 3	Line 4	Line 5	Line 6	Line 7
P(MW)	9608	13190	8949	5405	14810	958	635	1581	439	2016	3195	1196

3 AC network admittance measurement

3.1 Network admittance measurement method

As previously described, frequency sweep is used to extract the network admittance using RSCAD simulation at the connection point. As the MMC is modelled in the positive/negative sequence (PN) frame, the network admittance is thus also measured in the PN frame. As shown in Figure 6, a three-phase voltage source $V_{p(a,b,c)}$ is connected in series to the measuring point and frequency sweep is carried out. The magnitude of the injected phase voltage is 8kV. The steady-state time-domain voltage and current waveforms, i.e. v_{pg} and i_{pg} are measured in RSCAD. The data is then exported to Matlab where Fourier analysis is carried out to calculate the voltage and current magnitudes and phases for each of the injected frequencies in the PN frame. Due to the possible coupling between the P and N axes components, the admittances of the network at one specific frequency can be given as

$$\begin{bmatrix} i_{pgP} \\ i_{pgN} \end{bmatrix} = \begin{bmatrix} Y_{pp} & Y_{pn} \\ Y_{np} & Y_{nn} \end{bmatrix} \begin{bmatrix} v_{pgP} \\ v_{pgN} \end{bmatrix} \tag{1}$$

where Y_{pp} and Y_{nn} are the “self” admittance of the P and N axes, respectively. Y_{pn} and Y_{np} are the “cross” admittance from N to P and from P to N, respectively.

To extract the 4 admittances, two sets of voltage and current measurements for each frequency are required and the admittances are calculated using

$$\begin{bmatrix} Y_{pp} & Y_{pn} \\ Y_{np} & Y_{nn} \end{bmatrix} = \begin{bmatrix} i_{pgP1} & i_{pgP2} \\ i_{pgN1} & i_{pgN2} \end{bmatrix} \begin{bmatrix} v_{pgP1} & v_{pgP2} \\ v_{pgN1} & v_{pgN2} \end{bmatrix}^{-1} \tag{2}$$

where subscripts 1 and 2 refer to the first and second measurements.

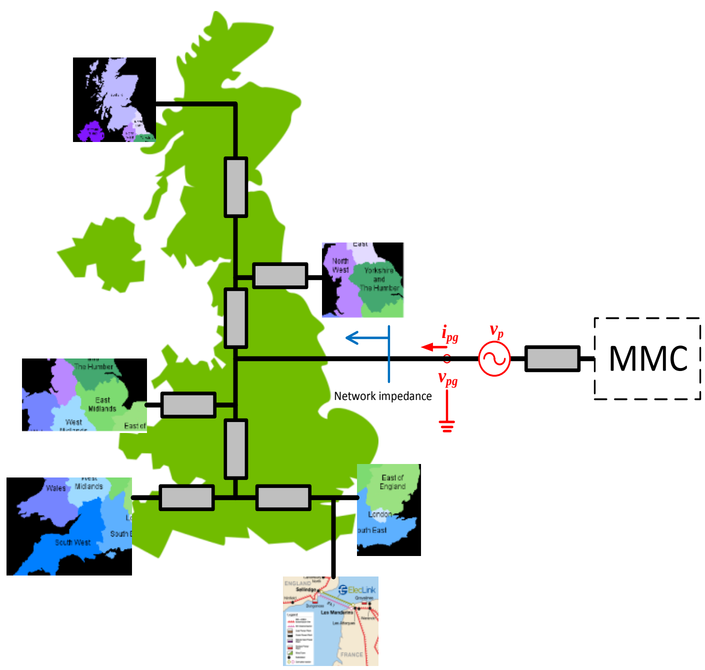

Figure 6 Injection of voltage for admittance measurement

3.2 The admittance of the AC grid model

Figure 7 (a) shows the measured positive sequence admittance Y_{pp} of the AC network at the connection point shown in Figure 5. The negative sequence admittance Y_{nn} has similar shape as Y_{pp} and thus not shown here. When the injected frequency closes to 50Hz during frequency sweep, i.e. close to the nominal operation frequency, the nominal operating condition can affect the measurement accuracy of the voltage and current at such frequency and consequently, leads to small errors of the admittance measured, especially on the phases. As can be seen, for the specific AC network model investigated, the measured admittances are largely inductive.

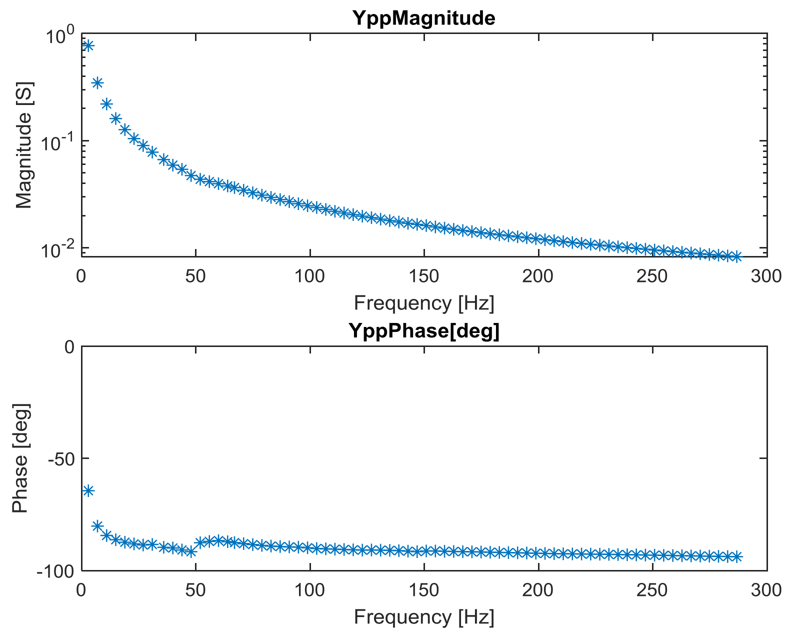

(a) Y_{pp}

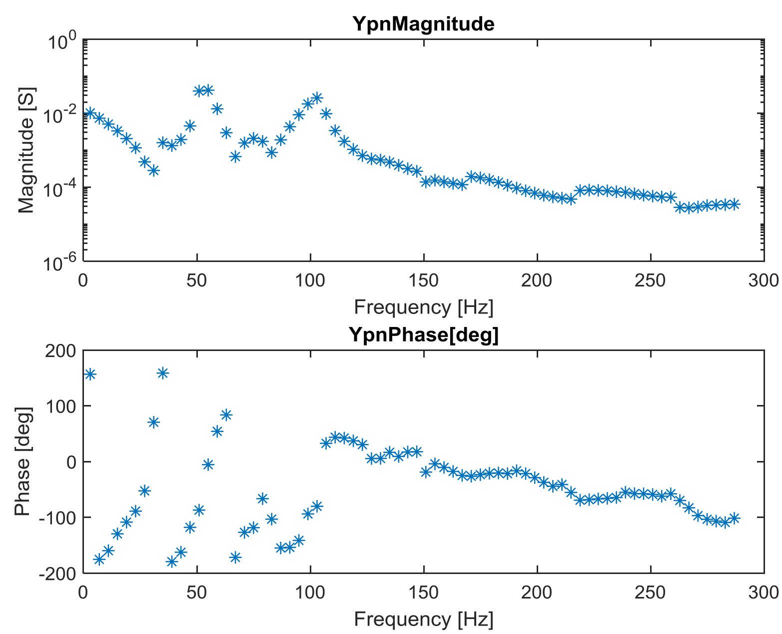

(b) Y_{pn}

Figure 7 Measured network admittance seen at the MMC terminal (excluding the connection cable)

Figure 7 (b) shows the measured coupling admittance Y_{pn} of the network whilst Y_{np} has similar shape as Y_{pn} and thus not shown here. It can be seen from Figure 7 (b) that the magnitude of Y_{pn} is much smaller than that of Y_{pp}, indicating weak admittance cross coupling between the P and N axes for the AC network model. The large phase variations of Y_{pn} as shown in Figure 7 (b) is due to the measurement error. This is due to the fact that the introduced coupling voltages and currents are all small and thus even a very small error can lead to large phase variation.

From the admittance shown in Figure 7, it can be observed that the dynamics of the synchronous generators and their controls do not affect the admittances of the system seen at the connection point. This is largely due to the fact that their impact frequency (below ten hertz) is much lower than the frequency of interest for converter stability (from tens hertz to hundreds hertz). The AC network admittance appears similar to a purely inductive network.

4 Load modelling and its impact on grid admittance

The loads in the existing RSCAD AC grid model are of constant power type. Further studies are carried out to investigate impact of different load representations widely used in power system studies on grid admittance.

4.1 Load modelling method

In the simplest form, loads may be represented by fixed shunt passive elements. Resistive, inductive, and capacitive shunt branches may be placed at a bus to represent active and reactive loads. Other components which may be used to model loads include the source model with fixed magnitude and phase, the induction machine model, the static load model and the dynamic load model [7].

Dynamic single phase and three-phase load models exist in RSCAD power system component library to represent different loads in the power network. The dynamic models can be used to adjust the load to maintain active and reactive power set points using a variable conductance. The load can be connected either in wye or delta configuration and modelled as series resistance and reactance (R-X) or parallel (R//X) connection. The power set points can be controlled using either sliders, control components or ZIP components, as shown in Figure 8.

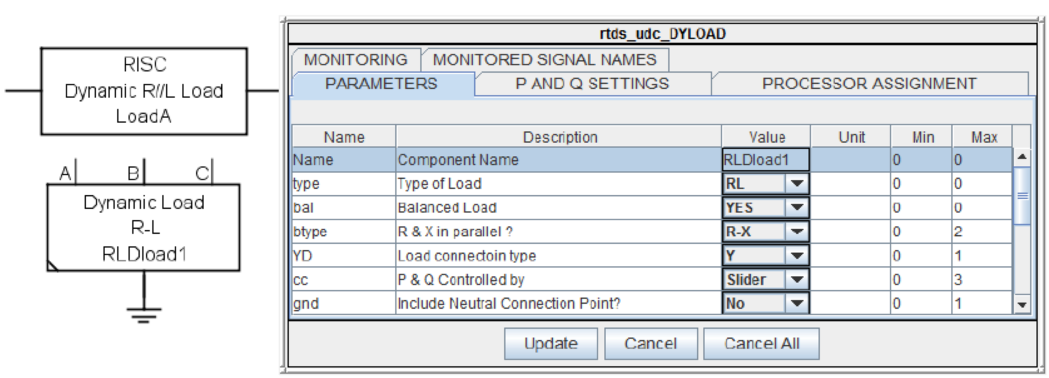

Figure 8 Load model in RSCAD

In this study, four load models provide by RSCAD are considered:

- Constant power load which dynamically adjusts the conductance to maintain constant active and reactive power during voltage and frequency variations.

- Polynomial load which represents the relationship between power and voltage magnitude as a polynomial equation as

$$P_{ord} = P_{set} \times (a_1 U^{n_1} + a_2 U^{n_2} + a_3 U^{n_3}) \quad (3)$$

$$Q_{ord} = Q_{set} \times (a_4 U^{n_4} + a_5 U^{n_5} + a_6 U^{n_6}) \quad (4)$$

  where a_1-a_4 and n_1-n_4 are constants set by users. P_{ord} and Q_{ord} are then used as inputs for constant power load.

- ZIP load which is consisted of 20% constant admittance load (constant Z), 40% constant current load (constant I) and 40% constant power load (constant P).

- Exponential load which represents the relationship between power and voltage magnitude as exponential equations as

$$P_{ord} = P_{set} \times U^{np} \quad (5)$$

$$Q_{ord} = Q_{set} \times U^{nq} \quad (6)$$

  where *n* and *p* are constants set by users. P_{ord} and Q_{ord} are then used as inputs for constant power load.

For the constant power load, the time constant setting for R, L, C values is 0.01 seconds, based on measured bus voltage (RMS value). For the Polynomial/Exponential/ZIP loads, the time constant of bus voltage measurement for calculating the load power using the polynomial/Exponential/ZIP equations is also set at 0.01 seconds. Equally, the active and reactive power of the Polynomial/Exponential/ZIP loads are updated at every 0.01s. Figures 9 (a)-(d) show the way the four different types of loads are implemented in RSCAD.

The grid admittances applying different load models are measured and it is found that the four different load models present almost identical results as those shown in Figure 7 with the constant power load. This is due to the large time constant of 0.01s used in the load models in RSCAD simulations which means as variation of high frequency components in the network will not be reflected in the dynamic response of the system.

From this study, it can be concluded that the traditional method used for load modelling does not provide adequate dynamic response required for frequency domain converter interaction analysis. If there are unconventional load/generation (e.g. converter based) connected in close vicinity to converter stations and their dynamics could affect converter system stability, it is probably necessary for such load/generation to be modelled in details rather than using the generic representation.

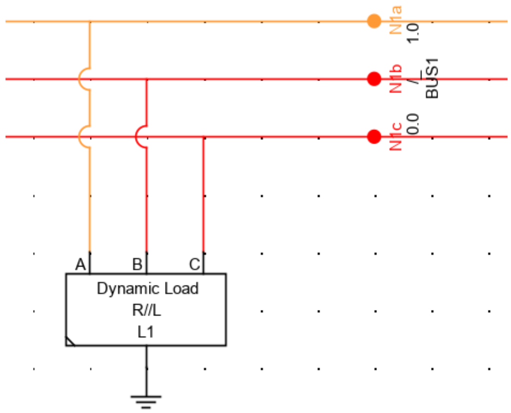

(a) Constant power load model

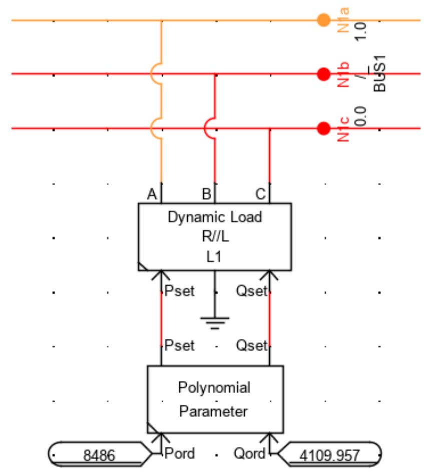

(b) Polynomial load model

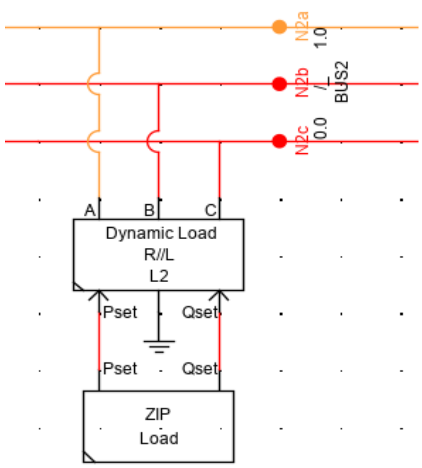

(c) ZIP load model

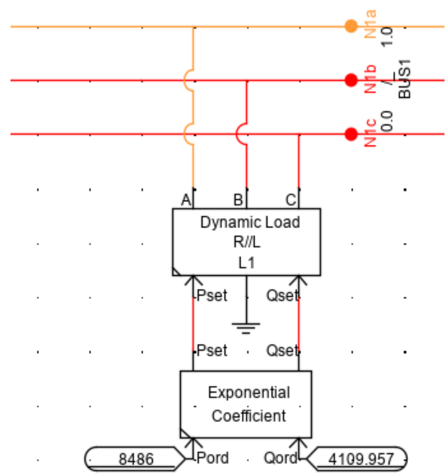

(d) Exponential load model

Figure 9 Load model in RSCAD implementation

5 Cable modelling and its impact on grid admittance

For network impedances seen by converters, they can be significantly affected by the existence of long cables in the network especially the natural resonant frequencies of typical AC cables are in the frequency range of interest for converters. Therefore, the existence of AC cables close to HVDC converters can potentially have significant impact on system stability. In this section, various cable modelling methods are explored and their impact on network impedance is assessed considering different cable lengths.

5.1 Cable modelling method

To capture the true dynamics of AC cables, the frequency dependant model is adopted in this study and used as a benchmark. The structure and parameters of the AC cable originated from the EU H2020

PROMOTioN project are given in Figure 10 and Table 5, respectively. Based on these physical parameters and materials, the AC cable is modelled in RTDS using Cable_V2 tool, as depicted in Figure 11.

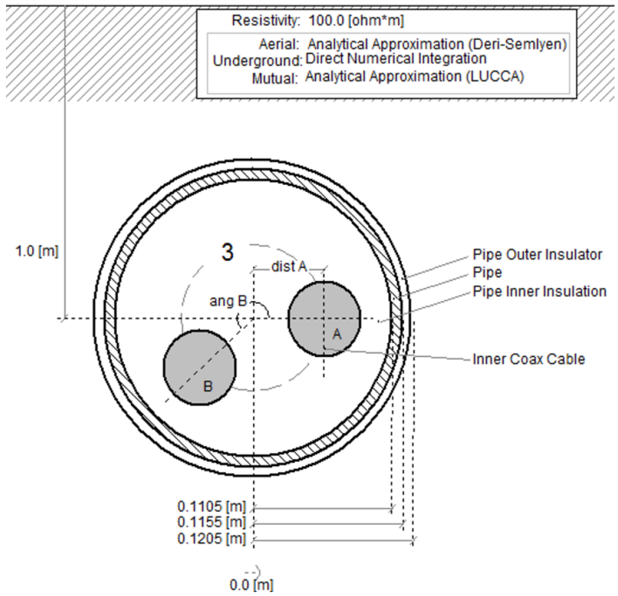

Figure 10 AC cable structure

Table 5 Cable parameters from the PROMOTioN Project

Parameters	**Value**
Power	400 MW
Frequency	50 Hz
Rated voltage	220 kV
Maximum admissible voltage	245 kV
Conductor cross-section	1000 mm^2
Conductor material	Copper
Insulation material	XLPE
Armour material	Steel
Diameter of conductor	37.9 mm
Insulation thickness	23.0 mm
Diameter over insulation	87.3 mm
Lead sheath thickness	3.1 mm
Outer diameter of the cable	241.0 mm
Capacitance	0.19 μF/km
Charging current per phase at 50 Hz	7.4 A/km
Inductance	0.38 mH/km

It should be noted that the RTDS Cable model is limited to model the capacitive and inductive coupling within one single-phase concentric cable. Modelling of the electromagnetic coupling between parallel cables is not supported.

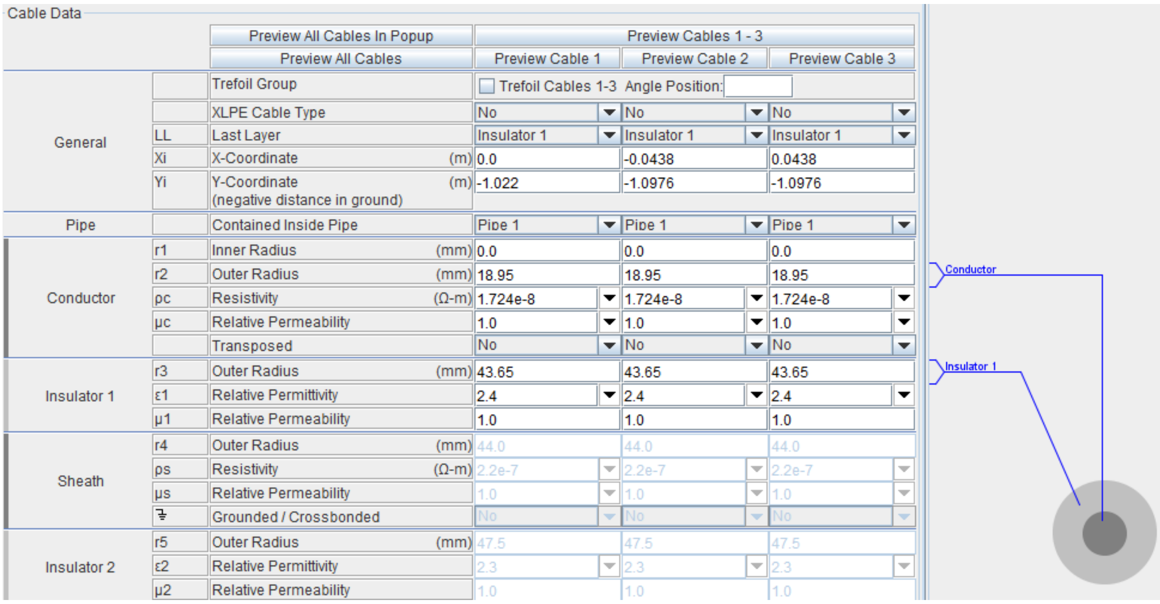

Cable Data

		Preview All Cables In Popup		Preview Cables 1 - 3		
		Preview All Cables		Preview Cable 1	Preview Cable 2	Preview Cable 3
General		Trefoil Group		Trefoil Cables 1-3 Angle Position:		
		XLPE Cable Type		No	No	No
	LL	Last Layer		Insulator 1	Insulator 1	Insulator 1
	Xi	X-Coordinate	(m)	0.0	-0.0438	0.0438
	Yi	Y-Coordinate (negative distance in ground)	(m)	-1.022	-1.0976	-1.0976
Pipe		Contained Inside Pipe		Pipe 1	Pipe 1	Pipe 1
Conductor	r1	Inner Radius	(mm)	0.0	0.0	0.0
	r2	Outer Radius	(mm)	18.95	18.95	18.95
	ρc	Resistivity	(Ω-m)	1.724e-8	1.724e-8	1.724e-8
	μc	Relative Permeability		1.0	1.0	1.0
		Transposed		No	No	No
Insulator 1	r3	Outer Radius	(mm)	43.65	43.65	43.65
	ε1	Relative Permittivity		2.4	2.4	2.4
	μ1	Relative Permeability		1.0	1.0	1.0
Sheath	r4	Outer Radius	(mm)	44.0	44.0	44.0
	ρs	Resistivity	(Ω-m)	2.2e-7	2.2e-7	2.2e-7
	μs	Relative Permeability		1.0	1.0	1.0
		Grounded / Crossbonded		No	No	No
Insulator 2	r5	Outer Radius	(mm)	47.5	47.5	47.5
	ε2	Relative Permittivity		2.3	2.3	2.3
	μ2	Relative Permeability		1.0	1.0	1.0

(a) Cable data

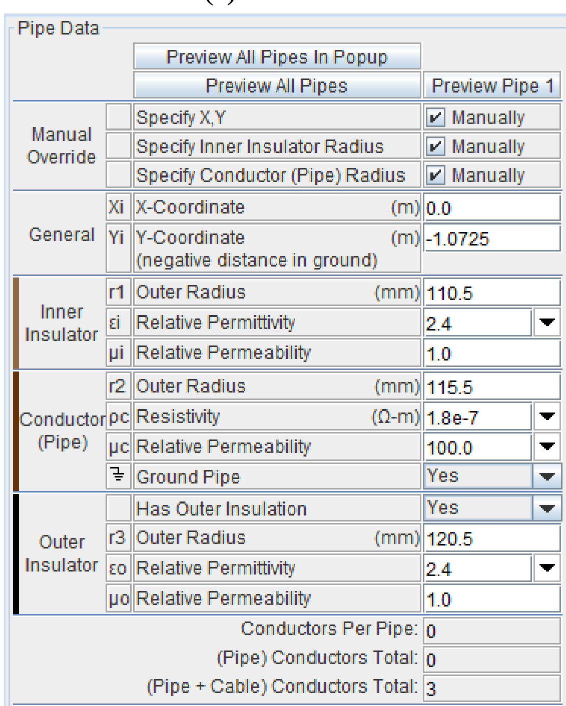

Pipe Data

		Preview All Pipes In Popup		
		Preview All Pipes		Preview Pipe 1
Manual Override		Specify X,Y		☑ Manually
		Specify Inner Insulator Radius		☑ Manually
		Specify Conductor (Pipe) Radius		☑ Manually
General	Xi	X-Coordinate	(m)	0.0
	Yi	Y-Coordinate (negative distance in ground)	(m)	-1.0725
Inner Insulator	r1	Outer Radius	(mm)	110.5
	εi	Relative Permittivity		2.4
	μi	Relative Permeability		1.0
Conductor (Pipe)	r2	Outer Radius	(mm)	115.5
	ρc	Resistivity	(Ω-m)	1.8e-7
	μc	Relative Permeability		100.0
		Ground Pipe		Yes
Outer Insulator		Has Outer Insulation		Yes
	r3	Outer Radius	(mm)	120.5
	εo	Relative Permittivity		2.4
	μo	Relative Permeability		1.0
		Conductors Per Pipe:		0
		(Pipe) Conductors Total:		0
		(Pipe + Cable) Conductors Total:		3

(b) Pipe data

Figure 11 Layout of AC cable model in RTDS

5.2 Impact of AC cables on grid admittance

After adding the AC cable between the simplified UK AC network and MMC, the grid admittance at the MMC connection terminal is measured. The measured Y_{pp} admittances for different cable lengths are shown in Figure 12 (a)-(d). It can be seen that the grid admittance changes after adding the cable. With a 20km cable added, the measured admittance remains largely inductive as previous case shown in Figure 7 (a). However, resonance appears at around 230Hz with a 60km cable. The resonant frequency is reduced to 170 Hz for a 100km cable and then further to 118Hz with a 180km cable. Such resonant frequencies are in the typical frequency ranges of MMC converter responses and potentially could significantly impact on system stability.

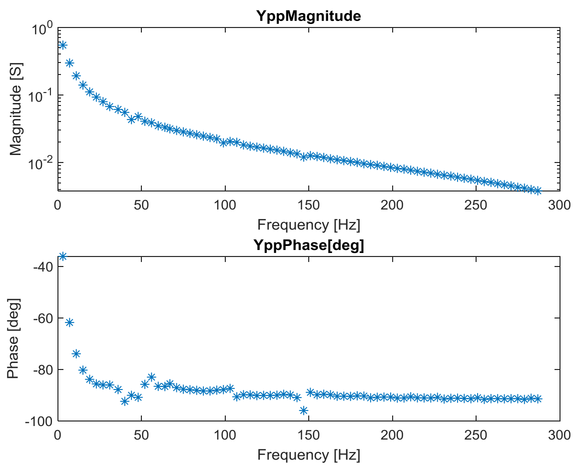

(a) 20 km AC cable
(no resonance)

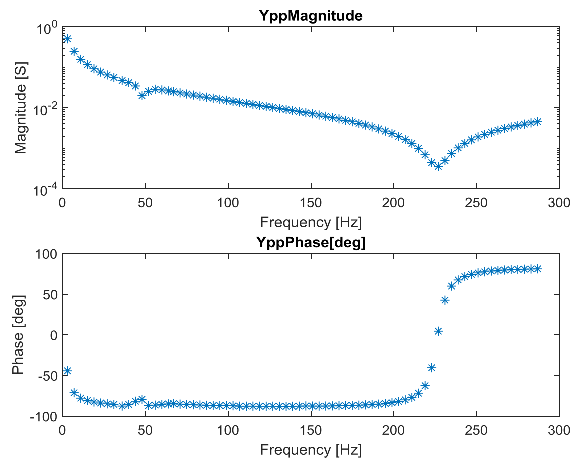

(b) 60 km AC cable
(resonance frequency is around 230Hz)

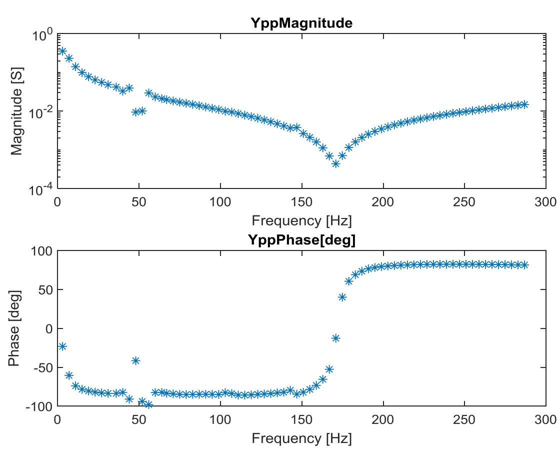

(c) 100 km AC cable
(resonance frequency is around 170Hz)

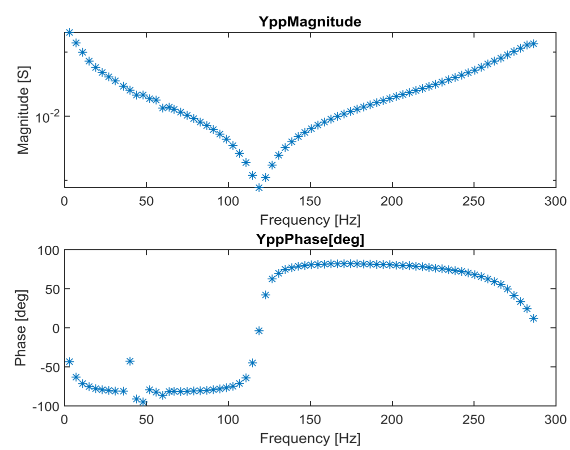

(d) 180 km AC cable
(resonance frequency is around 118Hz)

Figure 12 Grid admittance versus different cable length

5.3 Implementation of AC cable in analytical model

As can be seen in Table 5 and Figure 10, it is difficult to apply the physical parameters or frequency-dependent model of AC cable for analytical study. Therefore, it is necessary to find a simplified AC cable model, e.g. based on RLC values, which can still present accurate cable dynamic characteristics. According to CIGRE guidebook [9], a simplified pi-section model is established for a 60km AC cable based on the physical parameters, as shown in Figure 13. This lumped parameter model takes the following into account:

- Data related to the construction characteristics of the cable: layout (parallel single core cables and pipe type cables), geometry and properties of the conducting and insulating materials (conducting and insulating layers).
- Data related to the surrounding conditions (in air, buried directly underground, in ducts, troughs or in steel pipes).
- Skin and proximity effects for the calculation of AC resistance of conductors.
- Dielectric losses, screen and armour losses, losses in steel pipes, etc.

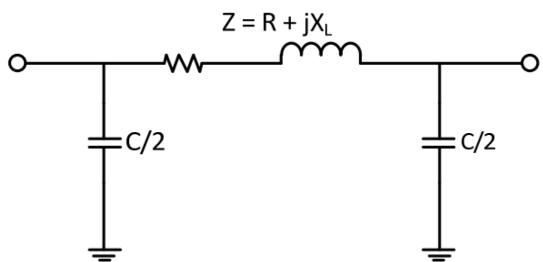

Figure 13 Equivalent 60 km AC cable model using RLC representation

I. Calculation of AC resistance (*R*)

The DC resistance of the conductor of the AC cable can be calculated as

$$R_{dc} = \frac{\rho_{20} l}{A} \tag{7}$$

where ρ_{20} is the resistivity of the solid copper conductor at 20 °C [Ωm]; *A* is the cross-sectional area of the conductor [m^2].

As the highest loss occurs at operating temperature 90 °C, the DC resistance used is modified as

$$R_{dc90} = R_{dc20}(1+\alpha(\theta\text{-}20)) \tag{8}$$

where R_{dc20} is the DC resistance of the conductor at 20 °C [Ω/m]. α is the temperature coefficient of copper at 20 °C per kelvin. θ is the maximum operating temperature in degrees Celsius. The AC resistance at 90 °C can be calculated as

$$R_{ac} = R_{dc90}(1 + y_s + y_p) \tag{9}$$

where y_s is the skin effect factor and y_p is the proximity effect factor.

II. Calculation of positive sequence impedance (Z_L)

The equivalent per unit resistance of the earth can be found as

$$R_e = \frac{\omega\mu}{8} \tag{10}$$

In (10), ω is the angular frequency [rad/s] and μ is the permeability of non-magnetic material, or vacuum. The depth of penetration for earth is

$$D_e = 659\sqrt{\frac{\rho_{earth}}{f}} \tag{11}$$

where ρ_{earth} is the resistivity of earth [Ω]. The reactance of the cable conductor per unit length is,

$$X_a = \frac{\omega\mu}{2\pi}\ln(\frac{D_e}{GMR_a}) \tag{12}$$

where GMR_a represents the geometric mean radius of core [m]. The reactance of the cable conductor per unit length is,

$$Z_L = R_e + R_{ac} + jX_a \tag{13}$$

III. Calculation of capacitance (C)

The capacitance of the cable is calculated by

$$C = 2\pi\varepsilon_r\varepsilon_0 / \ln(\frac{D}{d}) \tag{14}$$

where D is the external diameter of the main insulation (including outer semi-conducting layer) in mm. d is the diameter of the inner conductor (excluding first semiconducting layer) in mm. ε_r represents the relative permittivity of the insulation (assuming effective permittivity as 2.8). ε_0 represents the vacuum permittivity in F/m.

According to the parameters listed in Table 5 and Figure 10, the calculated grid admittances Y_{pp} with the 60km HVAC cable using lumped PI section model and frequency dependent model are compared in Figure 13.

From Figure 13, it can be seen that the lumped RLC model doesn't fit the frequency dependent model well. The resonance frequency using the lumped model is 174.5Hz while it is 226.8Hz using the frequency dependent model. It is caused by the use of simplified formulas with approximations, e.g. the depth of cable and actual cross-bonded configuration are not considered in the manual calculation. Additional measurements with increased PI sections using the calculated RLC model provide similar results as that of the single PI section model.

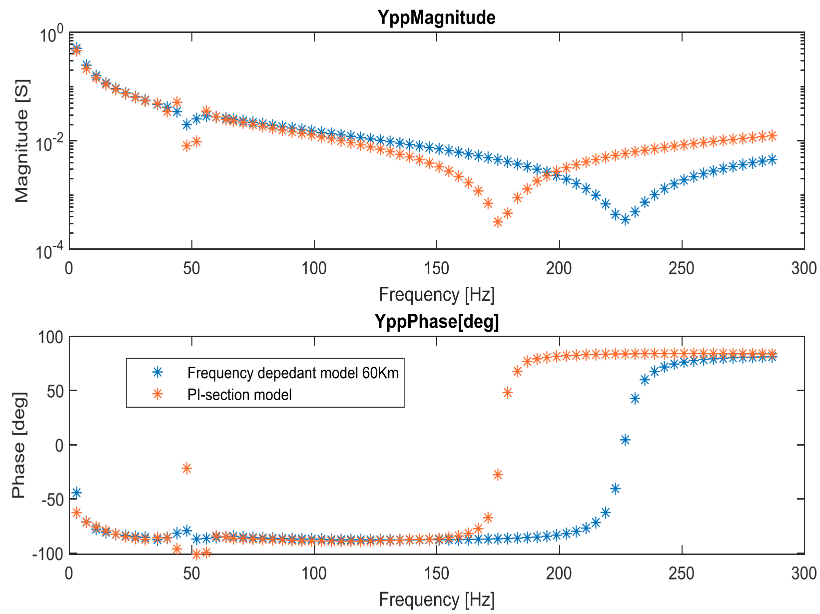

Figure 14 Comparison of Grid admittances with 60 km HVAC cable using lumped RLC PI section model and frequency dependent cable model

In order to obtain the lumped parameter model which can accurately represent the resonance frequency for analytical studies, the curve fitting method is applied to the RLC calculation method based on the CIGRE report. Considering the resonance in the grid caused by *LC* oscillations, the resonance frequency f_{FD} of the frequency dependant model can be approximately expressed as:

$$f_{FD} = \frac{1}{2\pi\sqrt{LC_{FD}}} \tag{15}$$

Similarly, the resonance frequency f_{PI} using the pi-section model can be approximately expressed as,

$$f_{PI} = \frac{1}{2\pi\sqrt{LC_{PI}}} \tag{16}$$

where the value of C_{PI} is calculated according to the CIGRE method as

$$C_{PI} = 2\pi\varepsilon_r\varepsilon_0 / \ln(\frac{D}{d}) \tag{17}$$

Based on (15-17), the revised capacitance used in the simplified PI section model is thus determined by,

$$C_{PI(new)} = C_{PI}\left(\frac{f_{PI}}{f_{FD}}\right)^2 \tag{18}$$

Using the measured resonant frequencies of 174.5Hz and 226.8Hz for the original PI section model and frequency dependent model, the equivalent $C_{PI(new)}$ is thus calculated using (18). Without changing the L and R values, the measured admittance using the revised lumped RLC model is depicted in Figure 15. As can be seen, the resonance frequency shown by the new pi-section model is almost in accordance with that from the frequency dependent model, and thus can be used for analytical study of converter system stability.

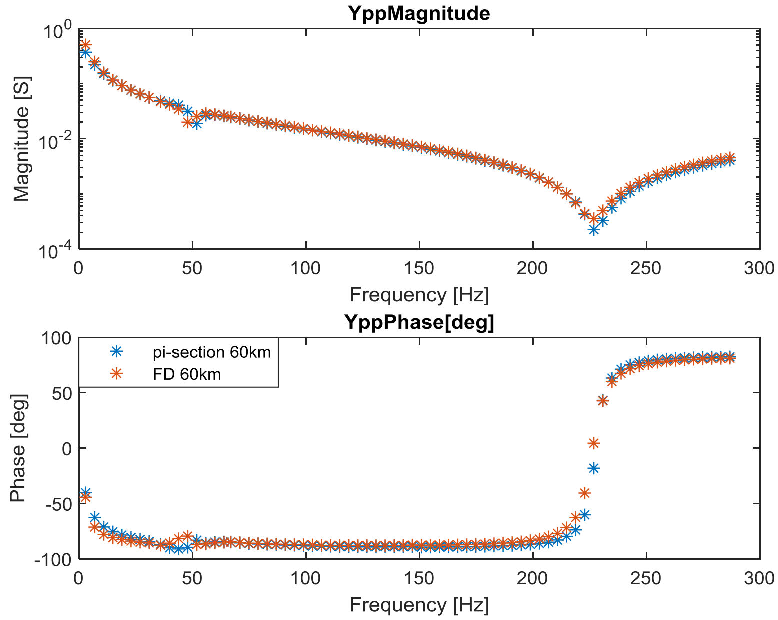

Figure 15 Grid admittance using the revised lumped RLC model

6 System configuration for converter interaction study

When multiple converters in close proximity are considered for studying converter interaction, shown in RED area in Figure 16 as an example, the network admittance seen at each of the converter connection points will need to be considered together with the electrical coupling between the converters. In order to perform analytical studies of system stability and interaction, a simplified network structure is thus constructed which can be quantified using the so-called multi-infeed interaction factor (MIIF) [10] between the converters.

Considering the case with two converters, each of the converter can be equivalent as connecting to a network through certain impedance whereas the two networks are also interconnected. Thus, a simplified network configuration as shown in Figure 17 (a) can be developed. Using MIIF to quantify converter interaction, the followings are considered:

- MMC1 infeed is considered as an existing HVDC link, and thus $X_{infeed1}$ can be pre-determined.
- For cases when there exists strong electrical coupling between MMC1 and MMC2, i.e. the two converters are in close proximity (or high MIIF), X_c is set to a low value while $X_{infeed2}$ is set to a high value so MMC2 can be considered as largely connected to S1 (e.g. S2 is further away from MMC2)

- For cases when there only exists weak electrical coupling between MMC1 and MMC2 (i.e. low MIIF), X_c is set to a high value while $X_{infeed2}$ is set to a low value so MMC2 can be considered as largely connected to S2.

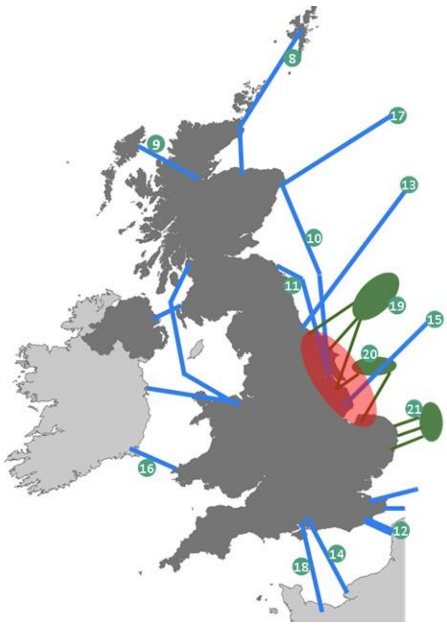

Figure 16 Example of multiple converters in close proximity

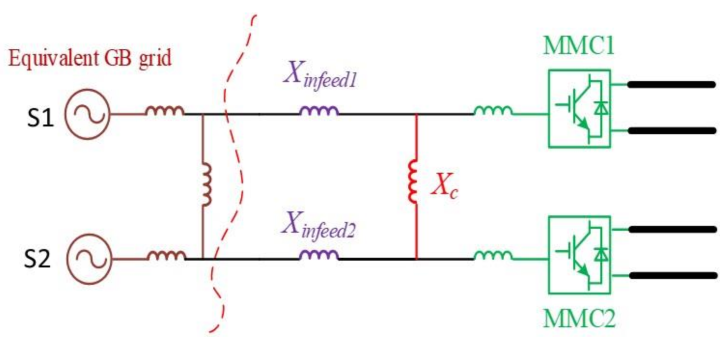

(a)

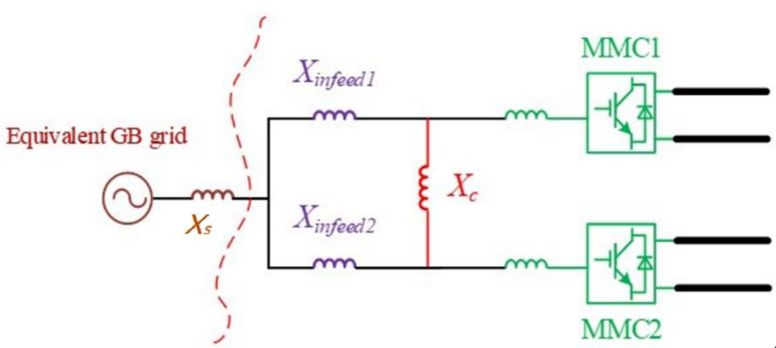

(b)

Figure 17 Equivalent circuit configuration for analytical studies

The two equivalent sources can be further simplified as one as shown in Figure 17 (b). The source impedance X_s can be set based on the network strength in the specific network area, e.g., based on the measured network impedance in Section 3. The three external network impedances (X_c, $X_{infeed1}$, $X_{infeed2}$) can be varied as described to represent the impedance of the network, and the electrical coupling between the two MMC connection points. Cables can be considered in part of network as required using the equivalent circuits developed in Section 5.3.

7 Conclusion

Based on the existing 8-bus simplified GB dynamic network model, the development of AC network models suitable for studying converter interaction is presented, and network impedances/admittances in the PN frame using frequency sweep in RSCAD time domain simulation are measured. It is shown that for the existing AC network model studied, the measured admittances in the PN frame are largely inductive with negligible cross coupling between the P and N axes. Grid admittances incorporating four load models are also compared and it shows that the four measured admittances present almost identical results due to the large time-step (0.01s) used in RSCAD simulation. This concludes that the modelling approaches in traditional power system studies, including generation, load, transmission line etc. do not capture the high dynamics required for converter stability studies. Therefore, if unconventional load/generation (e.g. converter based) is in close vicinity to the converter connection point which is selected for stability investigation, it is necessary for such load/generation to be modelled in details (rather than using the generic power system models).

The existence of AC cables which can significantly affect network impedance seen by converters needs to be closely examined. The frequency dependant AC cable model is adopted in RSCAD simulation and it is found that the AC cable length has great impact on the grid admittance. Resonances are observed for cable lengths of 60km, 100km and 180km for the particular case studied. With the increase of AC cable length, the resonance frequency decrease. Simplified PI section model using lumped RLC values suitable for frequency domain analytical study is investigated. However, it is found that using PI section based cable model with typical RLC values directly calculated from Cigre guidebook results in significant errors on measured network admittance compared to that using frequency dependent cable model. A simple but accurate AC cable PI section model is then proposed which modifies the calculated capacitance based on the observed resonant frequency error between the two cable models, for studying stability problem in analytical approach.

A simplified network structure which can be configured to adopt the concept of multi-infeed interaction factor (MIIF) is then proposed for investigating interactions between two converters.

8 Reference

[1] "GB National Electricity System Seven Year Statement", National Grid, 2011.

[2] "Electricity Ten Year Statement", UK Electricity Transmission, Nov. 2015.

[3] Real Time Digital Simulator Tutorial Manual (RSCAD version), Nov. 2014.

[4] P. Kundur, "Power System Stability and Control", *EPRI Power System Engineering Series*, (Mc Graw-Hill, New York), 1994.

[5] X. Jun. A. Dysko. "UK transmission system modelling and validation for dynamic studies", *4th IEEE/PES ISGT Europe (ISGT EUROPE)*, 2013.

[6] TR on Validation of Real-time User-defined MMC Models, *Strathclyde-UK National HVDC Centre collaborative research project*, TR ref. USTRATH-HVDC Centre-P1-002, August 2018.

[7] IEEE Task Force on Load Representation for Dynamic Performance. "Load Representation for Dynamic Performance Analysis." *IEEE Trans. on Power Systems*, Vol. 8, No. 2, pp. 472-482, May 1993.

[8] TR on Development and Validation of MMC Converter Admittance Models, *Strathclyde-UK National HVDC Centre collaborative research project*, TR ref. USTRATH-HVDC Centre-P2-001, Oct. 2019.

[9] CIGRE WG C4.502, "Power System Technical Performance Issues Related to the Application of Long HVAC Cables", Oct. 2013.

[10] S. Zhou, G. Qiao, C. He, W. Wang, and T. Liu, "Research on the Voltage Interaction of Multi-Infeed HVDC System and Interaction Factor", *Journal of Power and Energy Engineering*, No. 3, pp. 41-48, 2015